Electrochemical and Solid-State Letters, **13** (7) G57-G59 (2010)
1099-0062/2010/13(7)/G57/3/$28.00 © The Electrochemical Society

Bendable and Transparent Barium Titanate Capacitors on Plastic Substrates for High Performance Flexible Ferroelectric Devices

Kwi-Il Park, Sang Yong Lee, Seungjun Kim, Jaemyung Chang,* Suk-Joong L. Kang, and Keon Jae Lee[z]

Department of Materials Science and Engineering, Korea Advanced Institute of Science and Technology, Daejeon 305-701, Republic of Korea

This article describes a fabrication procedure of high performance flexible ferroelectric materials supported on plastic substrates and the characterization of $BaTiO_3$ thin films on flexible substrates. Ferroelectric $BaTiO_3$ thin film was deposited using radio-frequency magnetron sputtering on a $Pt/Ti/SiO_2/(100)$ Si substrate and annealed at 700°C for crystallization. The metal-insulator ($BaTiO_3$)-metal structure was successfully transferred onto flexible substrates by the standard microfabrication and soft lithographic printing methods after removing the underlying sacrificial TiO_2 layer by buffered oxide etchant etching. The dielectric constant of the $BaTiO_3$ thin films on the flexible substrate was comparable with that on a bulk Si substrate. No significant change in dielectric constant was observed upon bending with various radii and debending.
 [DOI: 10.1149/1.3407622]

Manuscript submitted February 25, 2010; revised manuscript received March 31, 2010. Published April 22, 2010.

Ferroelectric thin film materials, for example, ZnO,[1,2] polymers [poly(vinylidene fluoride) and polypropene],[3,4] and perovskite-type oxides (e.g., $BaTiO_3$, $PbZr_xTi_{1-x}O_3$, $SrBi_2Ta_2O_9$, $Ba_{0.5}Sr_{0.5}TiO_3$, and $BiFeO_3$) are being studied with great interest for various applications, such as thin-film capacitors, piezoelectric microactuators, tunable microwave devices, nonvolatile ferroelectric random access memories, and ferroelectric field effect transistors.[5-8] Among these ferroelectric materials, $BaTiO_3$ thin films have drawn considerable attention not only due to their excellent ferroelectric characteristics but also to their lead-free bio-eco-compatible material properties. Recently, research on printable, flexible, and stretchable technology has been quickly progressing,[9-12] in particular, on flexible ferroelectric devices using perovskite structures directly deposited on plastic substrates by, for example, aerosol deposition[13] and the hydrothermal method.[14] However, the low temperature ferroelectric thin films, even on bulk substrates, exhibit low dielectric constants with poor remnant polarization[15] and high loss factor,[16] making them unsuitable for high performance flexible applications. The laser annealing method of sol–gel coated $BaTiO_3$ film on flexible substrates is also being investigated.[17] However, laser technology is reported to cause a weight loss and to degrade ferroelectric properties due to the easy ablation, thin absorption depth, and high phase formation energy of the ceramic films.[18,19] These problems may be solved if we can prepare thin films on bulk substrates followed by high temperature thermal annealing and then transfer the films onto flexible substrates.

Microstructured semiconductor (μs-Sc) technology was incorporated with a high temperature process developed by the University of Illinois at Urbana-Champaign research group in 2004[20-23] for fabricating high performance flexible devices. The developed μs-Sc technology enables us to transfer single crystal semiconductor materials onto flexible substrates by carving out from the bulk wafer utilizing the standard microfabrication and soft lithographic printing technique. The advantage of this technique is that high temperature processes such as doping or ohmic contact on silicon wafers can be employed before transferring the device onto plastic substrates.

We describe herein a technique suitable for generating and printing a biocompatible microstructured $BaTiO_3$ thin film on plastic substrates. A $BaTiO_3$ thin film deposited on a $Pt/Ti/SiO_2/(100)$ Si substrate by radio-frequency (rf) sputtering was annealed at 700°C for crystallization and then transferred onto a flexible substrate using polydimethylsiloxane (PDMS) stamps to overcome the limitation appearing in the preparation of the conventional technique. The dielectric properties of $BaTiO_3$ on bulk wafers and flexible substrates were characterized, and a bending experiment was performed to test the mechanical stability on the plastic substrate.

Experimental

Figure 1a shows the schematics of the fabrication steps, which consists of the following steps: (*i*) deposition of a $BaTiO_3$ thin film on a $Pt/Ti/SiO_2/Si(100)$ substrate. The Si wafers (500 μm) were oxidized with a SiO_2 (150 nm) layer. Pt (120 nm) and Ti (20 nm) layers of the bottom electrode were obtained by an E-beam evaporator. A 320 nm $BaTiO_3$ thin film was deposited on a $Pt/Ti/SiO_2/Si$ substrate by rf magnetron sputtering at room temperature in an Ar atmosphere. Annealing at three different temperatures, 600, 700, and 800°C was carried out for the crystallization of the ferroelectric material. During the annealing process, Ti is oxidized to form a TiO_2 layer between the Pt and SiO_2 layers. (*ii*) Inductive coupled plasma–reactive ion etcher (ICP-RIE) etching of the metal-insulator-metal (MIM) structure. The $Au/BaTiO_3/Pt$ layers of the MIM structure were etched by chlorine gas based ICP-RIE etching using Al and plasma-enhanced chemical vapor deposited SiO_2 mask (300 × 100 μm). The sacrificial TiO_2 layer formed at the interface between the Pt and SiO_2 layers was removed using a buffered oxide etchant (BOE) for 20 s. (*iii*) Transfer of MIM structure onto plastic substrate. The PDMS stamp, inked with MIM capacitors, was placed on a polyurethane (PU)-coated plastic substrate (Kapton film, 125 μm thick) and PU was cured by UV light.[21] (*iv*) After peeling off the PDMS, the MIM capacitors were well settled on the plastic substrate. The final step of fabrication involved etching a portion of the $Au/Cr/BaTiO_3$ layers (see supplementary material for fabrication details of flexible $BaTiO_3$ capacitors, Fig. S1[24]).

The phases present in the thin films were characterized by X-ray diffractometer (XRD, Rigaku, D/MAX-IIIC, Tokyo, Japan) using Cu Kα radiation (λ = 0.15406 nm at 30 kV and 60 mA). Raman analysis (LabRAM HR UV/visible/near-IR, Horiba Jobin Yvon, France) was performed to provide a more comprehensive phase characterization of both bulk and flexible $BaTiO_3$ thin films using a 514.5 nm Ar^+ laser line as the excitation source. A scanning electron microscope (SEM, S-4800, Hitachi, Japan) was employed to observe the top and cross-sectional surfaces of the film. The dielectric properties of the $BaTiO_3$ capacitors were measured by an Agilent (Hewlett-Packard) 4284A Precision LCR meter under 5 mV at 1 kHz.

* Present address: Ceramic Group, Material Science, TU Darmstadt, Petersenstr. 23 64287 Darmstadt, Republic of Germany.
[z] E-mail: keonlee@kaist.ac.kr

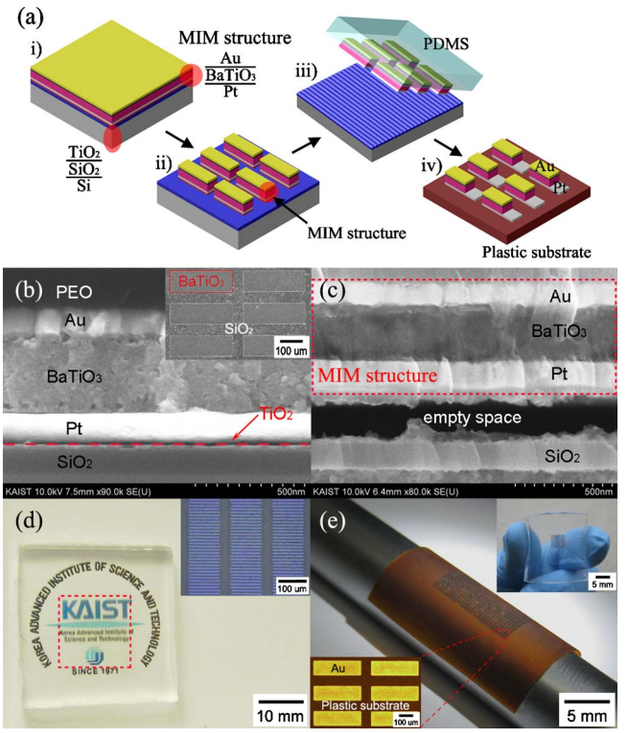

Figure 1. (Color online) (a) Schematic illustration of the process for fabrication of bendable $BaTiO_3$ capacitor on plastic substrate. (b) A cross-sectional image of the PEO/Au/$BaTiO_3$/Pt/TiO_2/SiO_2/Si structure. The inset shows the SEM image of $BaTiO_3$ top surface on oxidized Si substrates. (c) A cross-sectional view of sample in which TiO_2 sacrificial layer is etched by BOE for 20 s. MIM layers and SiO_2 layer are separated. (d) Photograph and magnified optical image of ITO-based transparent $BaTiO_3$ capacitors on PDMS. (e) The MIM capacitors supported on a plastic substrate around an aluminum rod after the capacitors on PDMS stamp were transferred on a plastic substrate. A magnified optical image of a portion is shown in the bottom inset. The upper inset shows the PDMS stamp inked with MIM structures.

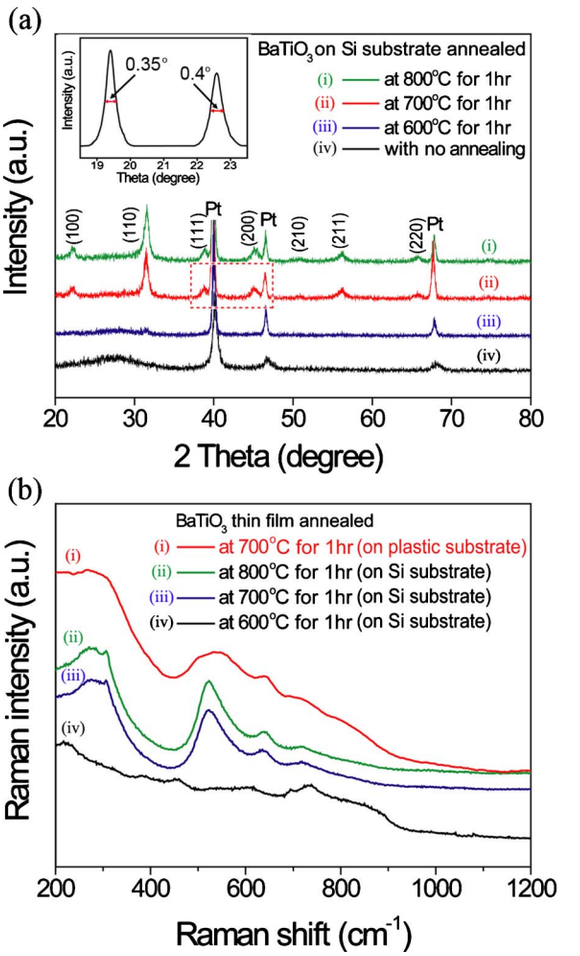

Figure 2. (Color online) (a) XRD patterns of $BaTiO_3$ thin film deposited on Pt/Ti/SiO_2/Si substrate by rf sputtering and annealed at different temperatures. The inset shows the X-ray rocking curve of $BaTiO_3$ (111) and (200) peaks. (b) Raman spectra of MIM structures deposited on Si substrate (black, blue, and green lines) and fabricated on plastic substrates (red line).

Results and Discussion

Figure 1b and c shows cross-sectional SEM images of the MIM structure (Au/$BaTiO_3$/Pt) on a SiO_2/Si substrate, which were taken before and after BOE etching, respectively. The SEM image in the inset of Fig. 1b shows a dense and smooth surface of a typical $BaTiO_3$ thin film on a Si substrate with no cracks or large pores. As shown in Fig. 1c, the Pt and SiO_2 layers were separated as a result of etching out of the TiO_2 sacrificial layer by BOE etching. The SiO_2 layer was not etched during the short period BOE etching (20 s), whereas the TiO_2 layer was completely etched out. The fast interface etching of the TiO_2 layer appears to delaminate the Pt and SiO_2 layers. An apparent advantage of utilizing a TiO_2 sacrificial layer is that the Si wafer can be reused for cost efficiency without chemical mechanical polishing, unlike in previous investigations.[22,25] The indium tin oxide (ITO)-based $BaTiO_3$ capacitors (indicated by a red dotted box) transferred onto the PDMS were transparent, as shown in Fig. 1d, and a magnified view is in the inset. Figure 1e is a photograph of a plastic substrate with MIM capacitors (corresponding to Fig. 1a-iv) wrapped around an aluminum rod 9 mm in diameter, and an optical image of printed MIM structures on a PU-coated plastic substrate was magnified in the bottom inset. The upper inset shows the MIM structures on the PDMS stamp (corresponding to Fig. 1a-iii) before the capacitors were transferred on the plastic substrate.

Figure 2a shows the XRD patterns of the $BaTiO_3$ thin films on the Pt/Ti/SiO_2/Si substrate annealed at 600, 700, and 800°C in air. The $BaTiO_3$ thin film on a silicon substrate annealed at 600°C is mostly amorphous, whereas the samples annealed at 700 and 800°C are well crystallized. The inset shows the X-ray diffraction rocking curve of the (111) and (200) peaks of the $BaTiO_3$ thin film annealed at 700°C for 1 h. The full width at half-maximum of the (111) and (200) peaks are about 0.35 and 0.40, respectively, indicating a good crystallinity of the film.[26] Figure 2b shows the Raman spectra of the $BaTiO_3$ thin films on a Si substrate (black, blue, and green lines) after annealing at different temperatures and that of the $BaTiO_3$ thin film transferred on a plastic substrate after annealing at 700°C for 1 h (red line). [Before Raman characterization of the $BaTiO_3$ thin film on the plastic substrate, the top electrodes (Au/Cr) on the $BaTiO_3$ thin film were removed.] The spectra of about 305 and 720 cm^{-1} were attributed to the A_1 and E (longitudinal optical) modes, specific to a tetragonal phase of $BaTiO_3$.[5] The XRD and Raman shift results indicate that the $BaTiO_3$ thin films on both bulk and flexible substrates have good crystallinity with a ferroelectric tetragonal phase;[5,26] however, the degree of $BaTiO_3$ crystallinity was changed after the BOE (containing HF) etching.

The dielectric properties of the films on Si and plastic substrates were measured. Without annealing, the dielectric constant was low ($\varepsilon_r < 20$), possibly because of the lack of tetragonal phase formation. Figure 3a shows the room-temperature dielectric constant (solid lines) and loss tangent (dotted lines) of high temperature

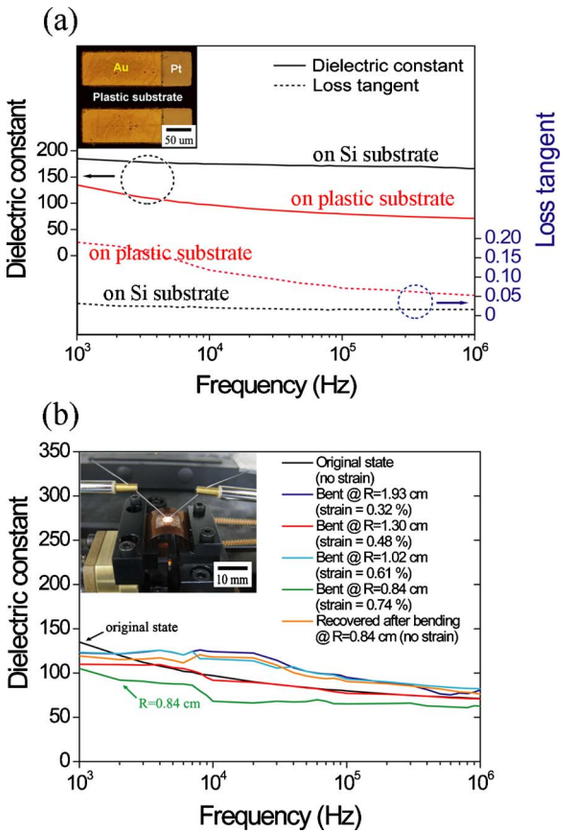

Figure 3. (Color online) (a) Dielectric properties of MIM structured $BaTiO_3$ thin film as a function of frequency on both Si and plastic substrates. The inset shows the optical image of the actual devices fabricated on plastic substrates. (b) Dielectric properties of $BaTiO_3$ thin film on plastic substrate at different bending radii and their corresponding strains. The inset shows the optical image of mechanical bending stage.

(700°C) annealed $BaTiO_3$ thin films on Si (black line) and plastic substrates (red line) as a function of frequency between 1 kHz and 1 MHz under 5 mV. The dielectric constant and loss tangent of a $BaTiO_3$ thin film on a Si substrate are 185 and 0.03, respectively, at a frequency of 1 kHz and slowly decrease with increasing frequency. These values and behavior are similar to those reported for MIM structured-$BaTiO_3$ thin films (ε_r = 115–318).[5,7,8,27]

The dielectric constant of a $BaTiO_3$ thin film on a plastic substrate (an optical image of the actual device in the inset of Fig. 3a) is 137 at 1 kHz, which is ~25% less than that on a Si substrate. This degradation is probably due to the removal of the glassy phases of $BaTiO_3$ during short BOE wet etching. Another possibility is the release of in-plane stresses during the detachment of the MIM structure from the Si substrate, as Shin et al. suggested.[28]

A mechanical bending test of the $BaTiO_3$ capacitors on plastic substrate was conducted using a bending stage, as shown in the inset of Fig. 3b. Figure 3b plots the dielectric constant curves with frequency at various bending radii (measured on the bending stage) and strains (calculated from the bending radius and the substrate thickness[21]). For the change in the bending radius (R) from 1.93 to 0.84 cm (corresponding from 0.32 to 0.74% of the surface strain), the dielectric constant does not appear to vary significantly upon bending. The dielectric constant of the device at a released state after a maximum bending exhibits essentially the same value as that without bending. These results demonstrate that our $BaTiO_3$ thin film is mechanically stable on a plastic substrate and has reasonable dielectric properties, although there is a need for improving the loss property.

Conclusion

We have developed a fabrication technique for ferroelectric, in particular, $BaTiO_3$ capacitor films on plastic substrates using microfabrication and soft lithography methods. To transfer the $BaTiO_3$ capacitor onto a plastic substrate, a metal oxide (TiO_2) sacrificial layer was introduced between the Si substrate and the MIM structure. The MIM structures on flexible substrates had dielectric constants comparable to that of $BaTiO_3$ thin film on a Si substrate and high mechanical stability upon harsh bending. The integration of flexible microstructured-ferroelectric materials utilizing the present technique may also provide innovative opportunities for designing flexible oxide based-piezoelectric materials for sensing devices[10] or energy harvesting systems.[2]

Acknowledgments

This work was supported by the Basic Science Research Program (grant code: 2009-0068063, CAFDC-2010-0009903), Pioneer Research Center Program (grant code: 2009-0093758), and Fundamental R&D Program for Core Technology of Materials (grant code: R17-2008-005-01001-0) through the National Research Foundation of Korea (NRF) funded by the Ministry of Education, Science and Technology.

Korea Advanced Institute of Science and Technology assisted in meeting the publication costs of this article.

References

1. M. Y. Choi, D. Choi, M. J. Jin, I. Kim, S. H. Kim, J. Y. Choi, S. Y. Lee, J. M. Kim, and S. W. Kim, *Adv. Mater.*, **21**, 2185 (2009).
2. R. S. Yang, Y. Qin, L. M. Dai, and Z. L. Wang, *Nat. Nanotechnol.*, **4**, 34 (2009).
3. I. Graz, M. Kaltenbrunner, C. Keplinger, R. Schwodiauer, S. Bauer, S. P. Lacour, and S. Wagner, *Appl. Phys. Lett.*, **89**, 073501 (2006).
4. T. Ji, M. Kathiresan, S. Nair, S. Jung, V. Natarajan, R. M. R. Vishnubhatla, and V. K. Varadan, *Proc. SPIE*, **6528**, 65281P (2007).
5. A. D. Li, C. Z. Ge, P. Lu, D. Wu, S. B. Xiong, and N. B. Ming, *Appl. Phys. Lett.*, **70**, 1616 (1997).
6. H. J. Chung, J. H. Kim, and S. I. Woo, *Chem. Mater.*, **13**, 1441 (2001).
7. B. Lee and J. P. Zhang, *Thin Solid Films*, **388**, 107 (2001).
8. K. M. Ring and K. L. Kavanagh, *J. Appl. Phys.*, **94**, 5982 (2003).
9. D. H. Kim, J. H. Ahn, W. M. Choi, H. S. Kim, T. H. Kim, J. Z. Song, Y. G. Y. Huang, Z. J. Liu, C. Lu, and J. A. Rogers, *Science*, **320**, 507 (2008).
10. T. Someya, T. Sekitani, S. Iba, Y. Kato, H. Kawaguchi, and T. Sakurai, *Proc. Natl. Acad. Sci. U.S.A.*, **101**, 9966 (2004).
11. K. J. Lee, M. J. Motala, M. A. Meitl, W. R. Childs, E. Menard, A. K. Shim, J. A. Rogers, and R. G. Nuzzo, *Adv. Mater.*, **17**, 2332 (2005).
12. B. A. Jones, A. Facchetti, T. J. Marks, and M. R. Wasielewski, *Chem. Mater.*, **19**, 2703 (2007).
13. Y.-C. Hu, C.-C. Hsiao, C.-M. Lee, and P.-C. Lin, in *Proceedings of the 4th Asia-Pacific Conference on Transducers and Micro-Nano Technology 2008 (APCOT 2008)*, National Cheng Kung University, Taiwan, ID0474 (2008).
14. R. Z. Hou, A. Y. Wu, and P. A. Vilarinho, *Chem. Mater.*, **21**, 1214 (2009).
15. B. S. Lee, S. C. Lin, W. J. Wu, X. Y. Wang, P. Z. Chang, and C. K. Lee, *J. Micromech. Microeng.*, **19**, 065014 (2009).
16. A. T. Chien, X. Xu, J. H. Kim, J. Sachleben, J. S. Speck, and F. F. Lange, *J. Mater. Res.*, **14**, 3330 (1999).
17. E. D. Tsagarakis, C. Lew, M. O. Thompson, and E. P. Giannelis, *Appl. Phys. Lett.*, **89**, 202910 (2006).
18. K. S. Seol, H. Hiramatsu, Y. Ohki, I. H. Choi, and Y. T. Kim, *J. Mater. Res.*, **16**, 1883 (2001).
19. Y. F. Zhu, J. S. Zhu, Y. J. Song, and S. B. Desu, *Appl. Phys. Lett.*, **73**, 1958 (1998).
20. E. Menard, K. J. Lee, D. Y. Khang, R. G. Nuzzo, and J. A. Rogers, *Appl. Phys. Lett.*, **84**, 5398 (2004).
21. K. J. Lee, J. Lee, H. D. Hwang, Z. J. Reitmeier, R. F. Davis, J. A. Rogers, and R. G. Nuzzo, *Small*, **1**, 1164 (2005).
22. K. J. Lee, M. A. Meitl, J. H. Ahn, J. A. Rogers, R. G. Nuzzo, V. Kumar, and I. Adesida, *J. Appl. Phys.*, **100**, 124507 (2006).
23. D. H. Kim, J. H. Ahn, H. S. Kim, K. J. Lee, T. H. Kim, C. J. Yu, R. G. Nuzzo, and J. A. Rogers, *IEEE Electron Device Lett.*, **29**, 73 (2008).
24. See supplementary material at http://dx.doi.org/10.1149/1.3407622 (E-ESLEF6-13-012007) for additional information.
25. A. J. Baca, M. A. Meitl, H. C. Ko, S. Mack, H. S. Kim, J. Y. Dong, P. M. Ferreira, and J. A. Rogers, *Adv. Funct. Mater.*, **17**, 3051 (2007).
26. C. L. Li, D. F. Cui, Y. L. Zhou, H. B. Lu, Z. H. Chen, D. F. Zhang, and F. Wu, *Appl. Surf. Sci.*, **136**, 173 (1998).
27. J. M. Zeng, H. Wang, M. Wang, S. X. Shang, Z. Wang, and C. L. Lin, *J. Phys. D*, **31**, 2416 (1998).
28. H. Shin, J. S. Park, S. Kim, H. S. Jung, and K. S. Hong, *Microelectron. Eng.*, **77**, 270 (2005).

Supporting Information for :

Bendable and Transparent Barium Titanate Capacitors on Plastic Substrates for High Performance Flexible Ferroelectric Devices

Kwi-Il Park[1], Sang Yong Lee[1], Seungjun Kim[1], Jaemyung Chang[1,a)], Suk-Joong L. Kang[1], and Keon Jae Lee[1]*

[1]Department of Materials Science and Engineering, Korea Advanced Institute of Science and Technology (KAIST), 373-1 Gwahangno, Yuseong-gu, Daejeon 305-701 Republic of Korea

*e-mail: keonlee@kaist.ac.kr, (Phone) 82-42-350- 3343, (Fax) 82-42-350-3310

For: Electrochemical and Solid-State Letters

[a)] Now, with Ceramic Group, Material Science, TU Darmstadt, Petersenstr. 23 64287 Darmstadt, Republic of Germany

Microfabrication and Soft lithography process

Figure S1 shows the schematics of the fabrication steps of the high performance flexible $BaTiO_3$ capacitors. The first step started with the deposition of a $BaTiO_3$ thin film on a $Pt/Ti/SiO_2/Si$ substrate using RF sputtering, followed by annealing for crystallization. During the annealing process, Ti is oxidized to form a TiO_2 layer between the Pt and the SiO_2 layers. Cr (10 nm) / Au (100 nm) layers were deposited on the annealed $BaTiO_3$ thin films to form a top electrode by RF sputtering [Fig. S1a]. A layer of 2.5 μm SiO_2 (PEO) was deposited by plasma enhanced chemical vapor deposition (PECVD, 400 mTorr, 50 SCCM 9.5 % SiH_4, 25 SCCM N_2O, 300 °C, 20W) and an aluminum (Al) thin film of 200 nm was obtained by RF sputtering.

To make a mask for the subsequent inductive coupled plasma-reactive ion etcher (ICP-RIE) etching, the Al (wet etching, AL-12 SK, CYANTEK Co.) and PEO (ICP-RIE etching, 25 mTorr, 40 SCCM CF_4, 150 W Power/40 W bias, 50 min) layer were patterned using the standard photolithography and etching technique [Fig. S1b]. $Au/Cr/BaTiO_3/Pt/TiO_2$ layers of MIM structure were also etched by chlorine gas based ICP-RIE etching (25 mTorr, 5 SCCM Ar/100 SCCM Cl_2, 400 W power/200 W bias, 20 min). The sacrificial TiO_2 layer formed[1, 2] at the interface between Pt and SiO_2 layers was removed using a buffered oxide etchant (BOE) for 20s [Fig. S1c]. The MIM capacitors were contacted with a polydimethylsiloxane (PDMS, Sylgard 184, Dow corning) stamp. Upon quick removal from the Si wafer, the rectangular shaped MIM capacitors were transferred to the elastomer [Fig. S1d]. The PDMS stamp, inked with MIM capacitors, was then placed on a plastic substrate (Kapton film, 125 μm in thickness) which was coated with polyurethane (PU, Norland optical adhesive, No. 73). UV light was then used to cure the PU [Fig. S1e]. After peeling off the PDMS, the MIM capacitors were well settled on the

plastic substrate. The residual PU and PEO layers on the plastic substrates were etched out by two subsequent oxygen RIE etching (50 mTorr, 100 SCCM O_2, 200 W, 8min) and fluorine gas based ICP-RIE etching (10 mTorr, 2 SCCM O_2/25 SCCM C_4F_8, 150 W power/40 W bias, 5min), respectively [Fig. S1f]. The final step of fabrication involved the patterning of PR on MIM structures to partially etch Au/Cr/$BaTiO_3$ layers [Fig. S1g] by wet etching of Au/Cr metal layers (Au/Cr etchant, Transene Inc.) and $BaTiO_3$ layers (H_2O : HF : HCl = 97 : 1 : 2, 20 s) [Fig. S1h].

REFERENCES

1. C. Hobbss, R. Hegde, B. Maiti, H. Tseng, D. Gilmer, P. Tobin, O. Adetutu, F. Huang, D. Weddington, R. Nagabushnam, D. O'Meara, K. Reid, L. La, L. Grove, and M. Rossow, 1999 Symp. VLSI Tech. Dig., Kyoto, Japan**,** 133 (1999).
2. K. Matsuo, K. Nakajima, S. Omoto, S. Nakamura, A. Yagishita, G. Minamihaba, H. Yano, and K. Suguro, Jpn J. Appl. Phys., **39**, 5794 (2000).

FIGURE CAPTIONS

S1. Schematic illustration of the process for fabricating of flexible $BaTiO_3$ capacitor. (a) Prepared MIM (Au/$BaTiO_3$/Pt) structures on Si substrate. (b) Rectangular pattern with Al/PEO mask (300 x 100 μm). (c) ICP-RIE etching of Au-$BaTiO_3$-Pt structure and BOE etching of TiO_2 layer between Pt and SiO_2. (d) Transfer of MIM capacitors to PDMS. (e) UV light exposure after contact of PDMS to PU coated-plastic substrates. (f) Peeling off PDMS and removing of residual PU and PEO using ICP-RIE. (g) PR pattern and partial removal of Au/Cr/$BaTiO_3$ layer for fabricating MIM capacitor devices on plastic substrates. (h) Removal of PR pattern and measurement of dielectric properties.

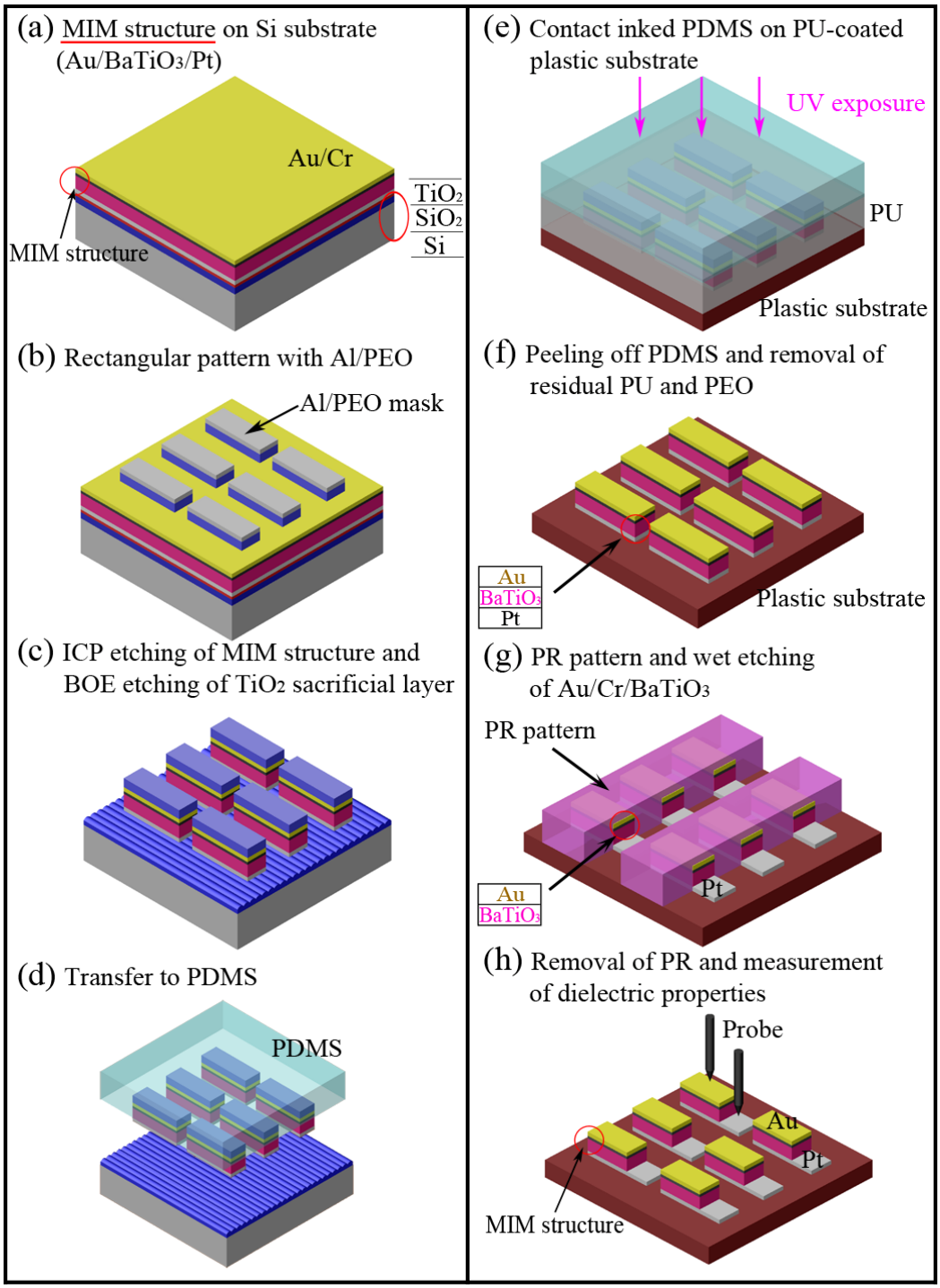
(a) MIM structure on Si substrate (Au/BaTiO3/Pt)
Au/Cr
TiO2
SiO2
Si
MIM structure
(b) Rectangular pattern with Al/PEO
Al/PEO mask
(c) ICP etching of MIM structure and BOE etching of TiO2 sacrificial layer
(d) Transfer to PDMS
PDMS
(e) Contact inked PDMS on PU-coated plastic substrate
UV exposure
PU
Plastic substrate
(f) Peeling off PDMS and removal of residual PU and PEO
Au
BaTiO3
Pt
Plastic substrate
(g) PR pattern and wet etching of Au/Cr/BaTiO3
PR pattern
Au
BaTiO3
Pt
(h) Removal of PR and measurement of dielectric properties
Probe
Au
Pt
MIM structure

Fig. S1